Journal of Naval Architecture and Marine Engineering
June, 2023
https://doi.org/10.3329/jname.v20i1.61155 *http://www.banglajol.info*

MHD CASSON AND CARREAU FLUID FLOW THROUGH A POROUS MEDIUM WITH VARIABLE THERMAL CONDUCTIVITY IN THE PRESENCE OF SUCTION/INJECTION

Babitha[1], C.V. Ramana Murthy[2] and G.Venkata Ramana Reddy[3]

[1]Department of Mathematics, Presidency University, Bangalore, India-560073, Email: babithaatiwale16@gmail.com
[2]Department of Engineering Mathematics, College of Engineering, Koneru Lakshmaiah Education Foundation, Andhra Pradesh, India-522302, Email: gvrr1976@kluniversity.in.
[3]Department of Engineering Mathematics, College of Engineering, Koneru Lakshmaiah Education Foundation, Andhra Pradesh, India-522302.,

Abstract:

The primary interest of this study is to investigate the results of magnetohydrodynamics Casson and Carreau fluid heat via a porous medium at the aspect of a stretching sheet. Variable thermal physical phenomena and suction/injection parameter results are also taken into account. Similarity transformations are applied to convert the governing equations of the magnetohydrodynamics Casson and Carreau fluid glide model into dimensionless non-linear normal differential equations. The results on velocity, concentration, temperature profiles, surface drag, Nusselt number, and Sherwood number are discussed for various flow parameters and presented the results through plots and tables. The fluid flow is analyzed for every suction and injection case. From the analysis it is noted that the velocity profile reduces by increasing the magnetic parameter and the reverse trend is observed for increasing values of Weissenberg number in the case of suction and injection. The temperature space and heat transfer rate enhances by increasing the variable thermal conductivity and more in the case of suction.

Keywords: Casson and Carreau fluid, suction.injection, variable thermal conductivity, magnetohydrodynamics, thermal radiation.

NOMENCLATURE

B_0	magnetic field (T)
C_p	specific heat $(J\ kg^{-1}K)$
q_r	Radiative heat flux
We	Weissenberg number
R	radiation parameter
D_{CT}	Soret kind diffusivity(m^2s^{-1})
M	magnetic parameter
k	thermal conductivity of the fluid
B_0	magnetic field (T)
C_p	specific heat $(J\ kg^{-1}K)$

Greek symbols

Γ	characteristic time constant
ν	kinematic viscosity (m^2s^{-1})
ϕ	dimensionless concentration
θ	dimensionless temperature
k^*	Rosseland mean absorption coefficient
μ	dynamic viscosity $(kg\ m^{-1}s^{-1})$
σ	electric conductivity $(\Omega^{-1}m^{-1})$
ρ	Density $(kg\ m^{-3})$
σ^*	Stefan-Boltzmann constant $(W\ m^{-2}K^4)$
γ	Casson fluid parameter

1. Introduction

Non-Newtonian fluids have drawn significant attention in recent decades on account of their tremendous applications in the fields of engineering, environment, and geophysics. Also, the study of non-Newtonian fluid motion and heat transfer past a stretching sheet has renewed great attention from several researchers due to its significance in many industrial and engineering applications, like liquid crystal solidification, exotic lubricants, wire drawing, fibers spinning, petroleum production, continuous cooling, and glass-fiber production, etc, In recent decades, several researchers (2016,2017,2018) reported their work on flow past a stretching sheet under various circumstances.

1813-8535 (Print), 2070-8998 (Online) Received on: Aug. 2022

The concept of magnetohydrodynamics (MHD) is adopted in the design of pumps, heat exchangers, space vehicles, thermal production, etc. Many researchers were interested in studying MHD non-Newtonian fluids flow through a permeable medium because of its potential uses in alloy and metal solidification, nuclear fuel debris treatment, and other fields ([2020,2021,2019,2020,2023,2022,2014]). In view of these applications and the importance of Soret together with Dufour on fluids that have a light molecular weight together with fluids with medium molecular weight, investigators have published many works whom Alam et al. (2005) examined the effects of Soret together with Dufour on free convection MHD as well as mass transport flow using numerical approach. Hasanuzzaman et al (2021) considered Soret together with Dufour on MHD unsteady mixed convection flow past a radiative porous vertical plate. Cheng (2011) has elucidated Soret together with Dufour's impacts on mixed convection heat together with mass transport through a downward-pointing vertical wall. Sharma et al. (2014) examine the impact of Soret together with Dufour on heat as well as mass transport for MHD mixed convection flow with Ohmic heating. The problem of mixed convective flow together with incompressible flow under the action of buoyancy as well as transverse magnetic field simultaneously in the presence of Soret and Dufour effects has been examined by Makinde (2011).

In the non-Newtonian fluids regime, a substantial amount of research has been done, and many more are needed in a range of non-Newtonian models. Since the power-law model is quite simple, few researchers are used to investigating non-Newtonian effects. However, due to the limits of the power-law model, this model has limitations, particularly for high and low shear rates. To investigate non-Newtonian effects, we can use various viscosity models. The Carreau fluid is a generalized Newtonian fluid in which fluid viscosity is dependent on shear rate. The Carreau fluid model is useful for describing fluid flow behavior at high shear rates. This model was first introduced by Pierre Carreau in 1972. Salman et al. (2018) have discussed the effect of variable thermal conductivity, and suction/injection on Carreau fluid flow past a stretching sheet. Under various conditions, the flow and heat transport characteristics of MHD Carreau fluid are examined by Shah et al.(2017). The flow and heat transport characteristics of MHD Carreau fluid past a permeable stretching sheet are studied by Reddy and Sandeep (2018) and they noted that Dufour and Soret parameters regulate the rate of heat and mass transfers. Madhura et al. (2022) have examined the effect of nonlinear thermal radiation on the MHD flow of micropolar Carreau fluid. Casson fluid is a plastic fluid that produces shear stress in constitutive equations. Soup, jelly, honey, paints, tomato sauce, coal in water, concentrated fruit juice, blood, and other fluid models are examples of Casson fluid models. Casson (1959) developed this model to estimate the flow behavior of printing ink pigment oil suspensions.

Priam and Nasrin (2022) have carried out a numerical study to examine the time-dependent peristaltic duct flow of four different Casson fluids and they noticed that 14.05% magnification of thermal distribution and 64.91% diminishment of total entropy due to rising internal thermal radiation from 0.5 to 2. Sohail et al. (2020) have analyzed the effect of variable thermal conductivity on MHD Casson fluid flow past a nonlinear stretching surface with entropy generation. The radiative heat transfer effect on a mixed convective flow of Casson fluid past a permeable sheet is discussed by Waqas et al (2017). The impact of couple stresses on mixed convective flow of Casson fluid through microchannel is studied by Felicita et al. (2016). Extensive researchers examined the nature of Casson fluid under various situations to analyze the flow and heat transfer characteristics (2020,2014, 2016). Raju and Sandeep (30) have examined the effect of nonlinear thermal radiation on the three-dimensional flow of Casson Carreau fluid in the presence of homogeneous–heterogeneous reactions.

The significance of non-Newtonian fluids flowing through a stretching sheet is explained by the literature review described above. In this study, the magnetohydrodynamics Casson and Carreau fluid (CCF) model was taken into account when analyzing the flow behavior. The primary goal of this work is to investigate the heat transfer properties of MHD CCF flow past a stretching sheet via a porous media. The study includes the effects of thermal radiation, fluctuating thermal conductivity, and suction/injection. The nonlinear dimensionless governing equations are numerically solved using the shooting method to examine how embedded parameters affect processes for mass, heat, and fluid transport. The findings are displayed using plots and tables.

2. Flow Analysis and Mathematical Formulation

Consider two-dimensional steady, MHD boundary layer flow of viscous, incompressible Casson and Carreau nanofluid over the heated permeable porous elongated sheet in the presence of chemical reaction were

examined. The sheet is taken into consideration within the x-axis with stretching velocity $u_w = ax$, wherein $a > 0$ is a constant. It was assumed that the flow of magnetic Reynolds variety is very small in liquid metals and partially ionized and the results of polarised prices are not taken into account. So, a prompted magnetic field is negligible in assessment with an applied magnetic area. The cartesian coordinate gadget has been utilized in a manner that the x-axis is along the stretching sheet, y-axis is ordinary to the sheet, the beginning is positioned at the space, and the flow inside the place is considered. The geometry of the drift phenomena is depicted in Fig-1.

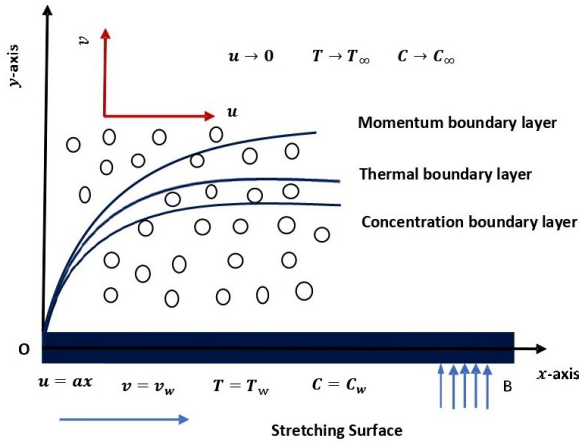

Fig-1. Schematic diagram of the flow

The governing equations for the fluid flow of the model are formulated as [2022]:

$$u_x + v_y = 0, \tag{1}$$

$$uu_x + vu_y = \nu\left(\left(1+\frac{1}{\gamma}\right)+\frac{3(n-1)}{2}\Gamma^2\left(u_x\right)^2\right)u_{yy} - \left(\frac{\sigma B_0^2}{\rho}+\frac{\nu}{K^*}\right)u, \tag{2}$$

$$uT_x + vT_y = \frac{1}{\rho c_p}\left(k(T)T_{yy}\right) - \frac{1}{\rho c_p}q_{ry} + D_{TC}C_{yy}, \tag{3}$$

$$uC_x + vC_y = D_{SM}C_{yy} + D_{CT}T_{yy} - Kr^*\left(C - C_\infty\right), \tag{4}$$

with the following boundary conditions that physically go along

$$\begin{aligned} u = u_w = ax, v = v_w, T = T_w, C = C_w \quad &\text{at} \quad y = 0, \\ u \to 0, T \to T_\infty, C \to C_\infty \quad &\text{as} \quad y \to \infty. \end{aligned} \tag{5}$$

In this study we incorporated the variable thermal conductivity, and it is expressed as $k(T) = k\left(1+\beta\left(\frac{T-T_\infty}{T_w-T_\infty}\right)\right)$.

In this analysis, the radiative heat flux is assumed to be $q_{ry} >> q_{rx}$ since the heat flux diverges only towards y-direction. Hence, the heat flux q_{ry} dominates the fluid flow. Considering that the difference in temperature throughout the flow is small in a way that T^4 is evaluated as a linear function of the ambient temperature T_∞. Simplifying T^4 in Taylor's approach in T_∞ and forgone terms of higher order to obtain:

$$T^4 \approx 4T_\infty^3 T - 3T_\infty^4. \tag{6}$$

Utilizing Rosseland approximation [26], the heat flux in terms y gives

$$q_r = -\frac{4\sigma_0}{3ke}\frac{\partial T^4}{\partial y}, \tag{7}$$

here σ_0 signifies Stefan-Boltzmann constant and ke signifies mean absorption coefficient. Since the Rosseland approximation is utilized in this analysis, the tangent hyperbolic liquid is assumed to be optically thick liquids. Linearizing the (7) above and utilizing the outcome on the energy equation to obtain

$$uT_x + vT_y = \frac{1}{\rho c_p}\left(k(T)T_{yy}\right) - \frac{16\sigma_0}{3\rho c_p ke}T_\infty^3 T_{yy} + D_{TC}C_{yy}\,. \tag{8}$$

The governing equations (2),(4),(8) and (5) are transformed into ordinary differential equations by introducing the dimensionless variables are given by :

$$\psi = \sqrt{av}xf(\eta),\ \theta(\eta) = \frac{(T-T_\infty)}{(T_w-T_\infty)},\ \phi(\eta) = \frac{(C-C_\infty)}{(C_w-C_\infty)},\ \eta = \sqrt{\frac{a}{v}}y. \tag{9}$$

The stream function velocity ψ can be defined as $u = \psi_y, v = -\psi_x$ so that equation (5) satisfies the continuity equation. $f(\eta)$ denote the injection and suction, η is the dimensionless space variable, $\theta(\eta)$ and $\phi(\eta)$ are the dimensionless of temperature and concentration of the fluid respectively.

In view of the above-mentioned transformations equations (2), (4) and (8) are reduced to the following ODEs:

$$\left(1+\frac{1}{\gamma}\right)f''' + ff'' - f'^2 + \frac{3(n-1)}{2}We\left(f''\right)^2 f''' - \left(M+\frac{1}{K}\right)f' = 0\,, \tag{10}$$

$$\left(1+\frac{4}{3R}\right)\theta'' + \Pr\, f\theta' + \beta\left(\theta\theta'' + \theta'^2\right) + \Pr\, Nd\phi'' = 0\,, \tag{11}$$

$$\phi'' + Le\phi' + \frac{Nd}{Ld}\theta'' - KrLe\phi = 0\,. \tag{12}$$

The transformed boundary restrictions as:

$$\begin{aligned} &f = S,\ f' = 1, \theta = 1, \phi = 1 \text{ at } \eta = 0,\\ &f' \to 0, \theta \to 0, \phi \to 0 \ \text{ as } \ \eta \to \infty. \end{aligned} \tag{13}$$

where f', θ and ϕ are the dimensionless velocity, temperature and concentration respectively, The prime denotes differentiation with respect to η.

where the physical parameters are:

$M = \frac{\sigma B_0^2 x}{\rho u_w}$ – Magnetic parameter, $K = \frac{K^* a}{vx}$ -Permeabelity parameter,

$\mathrm{N}_b = \frac{\tau D_B (C_w - C_\infty)}{v}$ - Brownian motion, $\mathrm{N}_d = \frac{\tau D_T (T_w - T_\infty)}{vT_\infty}$ – Thermoporetic parameter

$Le = \frac{v}{D_B}$ – Leiws number, $\Pr = \frac{v}{\alpha}$ – Pramdtl number, $R_{e_x} = \frac{ax}{v}$ – Reynolds number;

$\mathrm{R} = \frac{4\sigma^* T_\infty^3}{k^* K}$ – Radiation parmater.

The skin friction C_f , local Nusselt number Nu_x and Sherwood number Sh_x are the important physical quantities they can be defined as follows

$$C_f = \frac{\tau_w}{\rho u_w^2},\ Nu_x = \frac{xq_w}{k(T_w - T_\infty)},\ Sh_x = \frac{xq_m}{D_{SM}(C_w - C_\infty)}, \tag{14}$$

here

$$\tau_w = \mu\left(\left(1+\frac{1}{\gamma}\right)\frac{\partial u}{\partial y} + \frac{n-1}{2}\Gamma^2\left(\frac{\partial u}{\partial y}\right)^3\right),\ q_w == k\frac{\partial T}{\partial y},\ q_m = -D_{SM}\frac{\partial C}{\partial y}. \tag{15}$$

Using (9) and (12), the above quantities can be transformed form are:

$$C_f\,\mathrm{Re}_x^{\frac{1}{2}} = \left(\left(1+\frac{1}{\gamma}\right)f''(0) + \frac{n-1}{2}We\left(f''(0)\right)^3\right),\ Nu_x\,\mathrm{Re}_x^{\frac{-1}{2}} = -\left(1+\frac{4}{3R}\right)\theta'(0),\ Sh_x\,\mathrm{Re}_x^{\frac{-1}{2}} = -\phi'(0).$$

where $\mathrm{Re}_x = \frac{ax^2}{v}$ is the local Reynolds number.

3. Numerical Computation:

The non-dimensional governing boundary layer equations (10)-(12) subject to the boundary conditions of (15) are solved numerically by using the Runge-Kutta fourth-order method in conjunction with the shooting

technique. First, the higher-order non-linear differential equations have been converted into simultaneous linear differential equations of first order and are further transformed into the initial value problem and it is solved numerically by applying the Runge-Kutta fourth order along with the shooting technique. The Skin-friction, the Nusselt and the Sherwood numbers have been discussed in detail and various physical parameters have been illustrated graphically.

4. Validation:

Skin friction coefficient values for different Hartmann numbers are compared in Table 1 with the work presented by Salman et al. [5] for analyzing the accuracy of our results which are showing close agreement with each other.

5. Results and Discussion

The main goal of this research is to investigate and discuss a complete analysis of the steady, MHD boundary layer CCF flow past an infinite stretching sheet embedded with porous media. Similarity and shooting schemes were employed to obtain the solutions for velocity, temperature, and concentration profiles. Thermal radiation, suction/injection, and variable thermal conductivity effects are considered in the study. The variation of non-dimensional fluid motion, concentration, and temperature is discussed in detail for different physical parameter values, including the magnetic parameter, Weissenberg number, porous parameter, Carreau fluid parameter, Casson fluid parameter, radiation parameter, Prandtl number, chemical reaction parameter, modified Dufour parameter, and Dufour solutal Lewis number is discussed in detail. The variation in fluid flow, temperature, and concentration are observed for the two cases $S > 0$ and $S < 0$. In plots, $S > 0$ indicates the suction with the solid line, and $S < 0$ is for injection with dashed lines. Physically S is utilized to control the fluid flow in the channel. Figure 2 shows the impact of magnetic parameters on dimensionless velocity profiles for both cases of suction and injection. Increasing M values promote diminution in fluid flow for both cases. Physically M corresponds to Lorentz force because of which greater values of M enhance Lorentz force and this force is one type of resistive force acting against the motion of the fluid therefore fluid velocity decreases. In plots, the value of power law index n value is fixed as n=1.5 and n=1.6, because the considered CCF fluid is non-Newtonian. Generally, the power law index which categorizes the fluids into pseudo-plastic or shear thinning non-Newtonian for $n < 1$, Newtonian fluid for $n = 1$, and dilatant or shear thickening non-Newtonian fluid for $n > 1$. The range of physical parameters considered in this study is as follows: $0 \le M \le 4, 0.71 \le \mathrm{Pr} \le 7,\ 0 \le R \le 3, 0.1 \le Nd \le 0.5,\ 0.1 \le Ld \le 0.5,\ 0.1 \le \beta \le 3, 1 \le We \le 4,\ 0.1 \le \gamma \le 0.5,\ 0.1 \le Kr \le 2, -0.5 \le S \le 0.5, 0.5 \le K \le 4.$

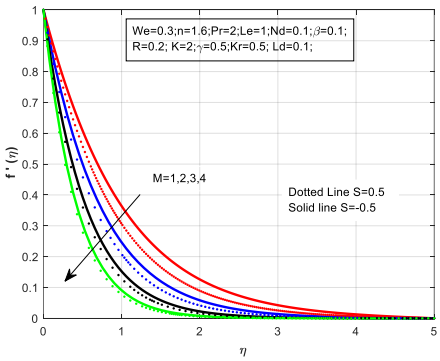

Fig. 2. Velocity profile versus magnetic parameter.

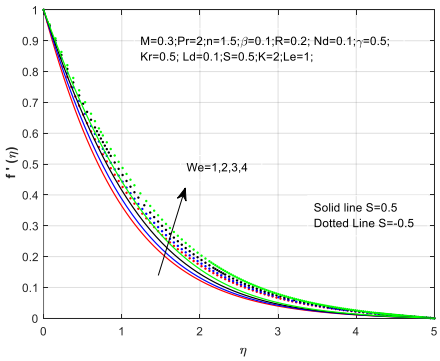

Fig. 3. Velocity profile versus Weissenberg number

The influence of the Weissenberg number We on the velocity profile is shown in Figure 3. The fluid motion improves as the Weissenberg number is increased. In terms of physics, the Weissenberg number is the ratio of relaxation time to fluid viscosity. The viscosity of the fluid decreases as the Weissenberg number rises, and the fluid motion rises as a result. The velocity profile is reversed when the porous parameter K is increased and is depicted in figure 4. The increase in the porosity parameter of the fluid is owing to an increase in the viscosity

of the fluid, or a drop in the permeability at the edge, or a decrease in the stretching rate of the accelerating surface, resulting in a progressive decrease in the fluid's flow velocity.

In Figure 5, the velocity profile is plotted against the Casson fluid parameter γ. Increased γ slowed the fluid flow in the direction of the stretching surface. This is because of the fall in yield stress at greater values of the γ which leads the fluid to behave more like a Newtonian fluid, resulting in a decrease in fluid velocity. Figure 6 shows the impact of the nonlinear thermal conductivity parameter β on the thermal profile. The temperature rises as a function of β. This is due to the fact that the higher the thermal conductivity, the higher the kinetic energy of the fluid particles, which raises the fluid temperature.

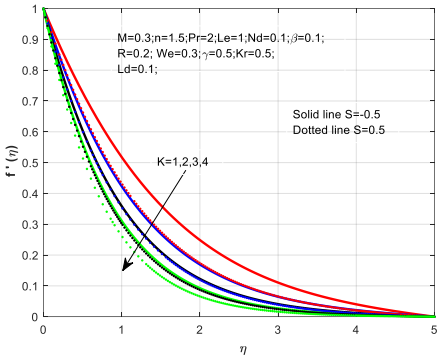

Fig. 4. Velocity profile versus porous parameter.

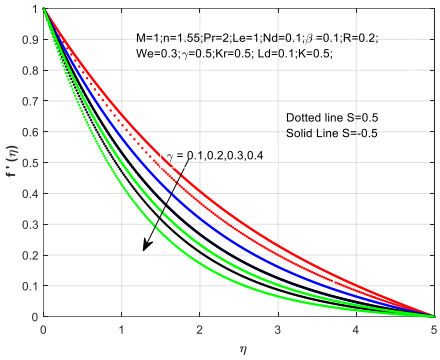

Fig. 5. Velocity profile versus Casson fluid parameter.

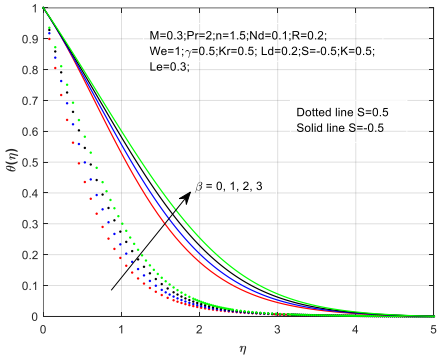

Fig. 6. Temperature profile versus thermal conductivity parameter.

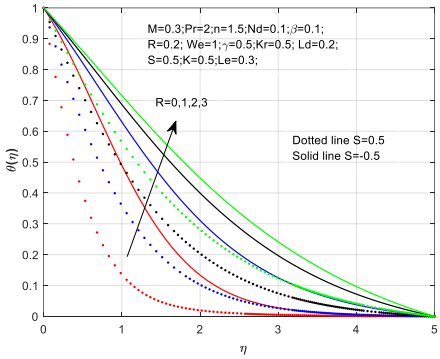

Fig. 7. Temperature profile versus radiation parameter.

Figure 7 displays temperature curves for various radiation parameter values. The radiation parameter R specifies how much conduction heat transfer contributes to thermal radiation transfer. It is evident that increasing the radiation parameter causes the temperature within the boundary layer to rise. Figure 8 depicts the impact of Prandtl's number Pr on the temperature field. The numerical results reveal that when the Prandtl number increases, the temperature decreases. A rise in the Prandtl number is associated with a decrease in the thickness of the thermal boundary layer and a lower average temperature within the boundary layer. Because lower Pr values imply higher thermal conductivities, heat can diffuse away from the heated surface more quickly than with higher Pr values. As a result, the boundary layer is thicker, and the rate of heat transmission is lowered in the case of smaller Prandtl numbers.

Figure 9 shows the impact of the Dufour number Nd on the fluid's temperature. Variation in the Dufour number has only minor effects on the fluid temperature, according to this diagram. The Dufour effect is magnified, which results in a modest increase in the fluid's temperature because the viscosity of fluid decreases and particles take momentum and the average temperature of fluid enhances and also noticed that the decrement in heat transfer rate. Since Dufour number and heat transfer rate are inversely related, i.e., $Nd \propto \frac{1}{T_w - T_\infty}$. So by rising Nd temperature gradient and thermal potential decays due to which heat flux reduction. Figure 10 depicts the effect of the Dufour solutal Lewis number Ld on the solute profile. With an increase in

the number of Dufour solutal Lewis, the solute distribution increased. Within the solute boundary layer, increasing the Ld increases the fluid concentration.

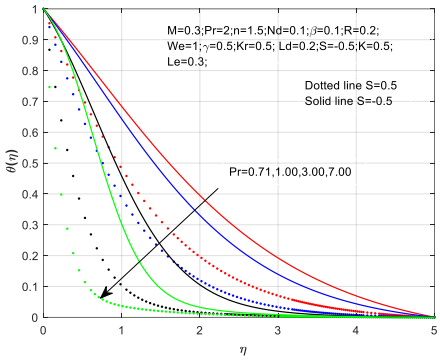

Fig. 8. Temperature profile versus Prandtl number.

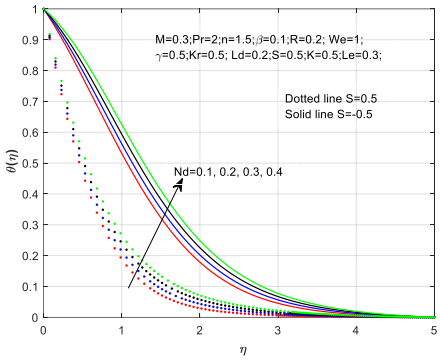

Fig. 9. Temperature profile versus modified Dufour parameter.

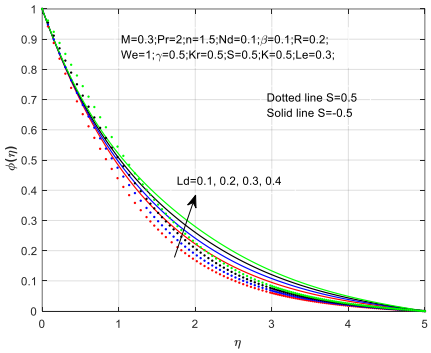

Fig. 10. Concentration profile versus Lewis number.

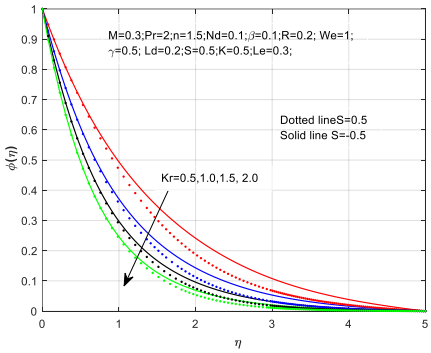

Fig. 11. Concentration profile versus chemical reaction parameter

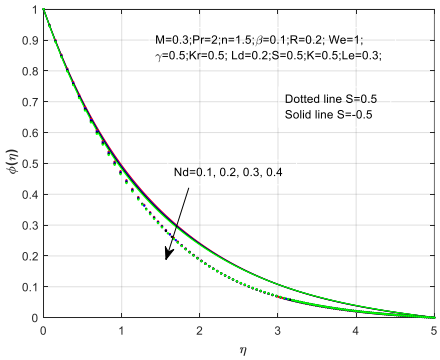

Fig. 12. Concentration profile versus modified Dufour parameter.

The influence of a chemical reaction parameter Kr on dimensionless concentration profiles is depicted in Figure 11. The concentration of the fluid is suppressed as the Kr is increased. Higher Kr values result in a decrease in chemical molecule diffusivity. As a result, they are obtained by species transfer. The species concentration decreases as Kr rises. With an enhancement in the Kr, the concentration distribution decreases at all places of the flow field. The influence of the Dufour solutal Lewis number Ld on concentration is shown in Figure 12. This parameter enhances the thickening of the solutal boundary layer while it reduces that fluid concentration.

Surface drag, heat, and mass transfer rates of the model are discussed in detail with the help of Tables 2-3. In point of physics, these quantities have great significance due to their vast applications in engineering and industrial fields. From Table 2, it is clear that surface drag is an increasing function of the magnetic parameter, Weissenberg number, porous parameter, and Casson fluid parameter. Heat and mass transfer rates are rises with the rise in thermal conductivity parameter, radiation parameter, and chemical reaction parameter, and heat transfer rate is decreasing function of modified Dufour number.

Table 1. Comparison of the skin friction for various values of M, and Pr = Nd = Ld = Le = We = n =γ=0

M	Salman et al.(2012)	Present Study
0	1.0000	1.00000
0.5	-1.1181	-1.118012
1	-1.4142	-1.414189

Table 2. Variation of friction drag for different values of $M, We, K,$ and γ

M	We	K	γ	S	Skin friction
1	0.3	2	0.5	-0.5	0.966957
2					1.355020
3					1.822203
4					2.309703
1				0.5	1.134600
2					1.516732
3					1.977366
4					2.457719
	1			0.5	0.698427
	2				0.764641
	3				0.847183
	4				0.939871
	1			-0.5	0.626586
	2				0.675865
	3				0.733013
	4				0.790057
		1		-0.5	0.609604
		2			0.815128
		3			0.981782
		4			1.124990
		1		0.5	0.785761
		2			0.986217
		3			1.149899
		4			1.290979
			0.1	0.5	0.448695
			0.2		0.604424
			0.3		0.716865
			0.4		0.803702
			0.1	-0.5	0.401367
			0.2		0.517181
			0.3		0.596134
			0.4		0.654575

Table 3. Impact of different physical parameters on heat and mass transfer rates:

β	R	Kr	Ld	Nd	S	Nusselt number	Sherwood number
0					0.5	0.855719	0.686429
1						0.954112	0.735279
2						1.10133	0.761286
0					-0.5	0.371158	0.699791
1						0.372821	0.69994
2						0.381621	0.700731
0.1	0	0.5	0.3	0.1	0.5	0.266182	0.705174
	1					0.287431	0.706006
	2					0.325364	0.70641
	0				-0.5	0.495053	0.746041
	1					0.610984	0.774109
	2					0.847285	0.812811
		0.5			0.5	0.29759	1.232912
		1				0.319851	1.259533
		1.5				0.345339	1.290779
		0.5			-0.5	0.704927	0.693342
		1				0.992564	0.996611
		1.5				1.215909	1.232086
			0.1		0.5	0.37583	0.700602
			0.2			0.376263	0.70267
			0.3			0.376662	0.704927
			0.1		-0.5	1.354313	0.511013
			0.2			1.342295	0.60333
			0.3			1.330601	0.693342

6. Concluding Remarks

MHD boundary layer flow, heat, and mass transport characteristic of CCF are studied numerically. Thermal radiation, suction/injection, and variable thermal conductivity effects are taken into account in the study. The significant outcomes of the study are drawn as follows:

- The fluid motion decreases for an enhancing value of the magnetic parameter, porous parameter, and time constant parameter, while intensifies for the Weissenberg number.
- The increase in thermal radiation parameter, variable thermal conductivity, and Dufour number leads to an increase in temperature in both suction and injection cases, on the other hand, fluid temperature decreases with an increase in Prandtl number.
- The fluid concentration decreases with an increase in chemical reaction parameter and increases with an increase in Dufour number and Dufour solutal Lewis number.
- The surface drag is intensifying with enhancing values of $M, We, K,$ and β.
- Heat transfer is an increasing function of variable thermal conductivity and thermal radiation and decreasing function of Dufour number.

Further, the impact of various physical phenomena on the CCF model can be discussed and also one can obtain the advantages of CCF flow through irregular channels in science concerning problems.

Acknowledgements

The authors are very much thankful to the Department of Mathematics, Presidency University, Bangalore and Department of Engineering Mathematics, College of Engineering, Koneru Lakshmaiah Education Foundation, Andhra Pradesh, for providing high-performance software for the computational work of this paper.

References

Alam, M. S., & Rahman, M. M. (2005). Dufour and Soret effects on MHD free convective heat and mass transfer flow past a vertical porous flat plate embedded in a porous medium. Journal of Naval Architecture and Marine Engineering, 2(1), 55-65.https://doi.org/10.3329/jname.v2i1.2030

Ali, M., Nasrin, R., & Alim, M. A. (2021). Analysis of boundary layer nanofluid flow over a stretching permeable wedge-shaped surface with magnetic effect. Journal of Naval Architecture and Marine Engineering, 18(1), 11-24. https://doi.org/10.3329/jname.v18i1.44458

Animasaun, I. L., Adebile, E. A., & Fagbade, A. I. (2016). Casson fluid flow with variable thermo-physical property along exponentially stretching sheet with suction and exponentially decaying internal heat generation using the homotopy analysis method. Journal of the Nigerian Mathematical Society, 35(1), 1-17. https://doi.org/10.1016/j.jnnms.2015.02.001

Babu, M. J., & Sandeep, N. (2016). MHD non-Newtonian fluid flow over a slendering stretching sheet in the presence of cross-diffusion effects. Alexandria Engineering Journal, 55(3), 2193-2201. https://doi.org/10.1016/j.aej.2016.06.009

Casson N, A flow equation for pigment oil suspensions of the printing ink type, In: Mill, C.C., Ed., Rheology of Disperse Systems, Pergamon Press, Oxford, 1959;84-102.

Channakote, M. M., & Kalse, V. D. . (2022). Combined convective and viscous dissipation effects on peristaltic flow of Ellis fluid in non uniform tube. Journal of Naval Architecture and Marine Engineering, 19(1), 1-12. https://doi.org/10.3329/jname.v19i1.55052

Cheng, C. Y. (2011). Soret and Dufour effects on natural convection heat and mass transfer near a vertical wavy cone in a porous medium with constant wall temperature and concentration. International communications in heat and mass transfer, 38(8), 1056-1060. https://doi.org/10.1016/j.icheatmasstransfer.2011.05.012

Felicita, A., Gireesha, B. J., Nagaraja, B., Venkatesh, P., & Krishnamurthy, M. R. (2023). Mixed convective flow of Casson nanofluid in the microchannel with the effect of couple stresses: irreversibility analysis. International Journal of Modelling and Simulation, 1-15. https://doi.org/10.1080/02286203.2022.2156974

Gurrampati, V. R. R., & Vijaya, K. (2022). The Buongiorno model with Brownian and thermophoretic diffusion for MHD casson nanofluid over an inclined porous surface. Journal of Naval Architecture and Marine Engineering, 19(1), 31-45. https://doi.org/10.3329/jname.v19i1.50863

Gurrampati, V. R. R., Ibrahim, S. M., & Bhagavan, V. S. (2014). Similarity transformations of heat and mass transfer effects on steady MHD free convection dissipative fluid flow past an inclined porous surface with chemical reaction. Journal of Naval Architecture and Marine Engineering, 11(2), 157-166. https://doi.org/10.3329/jname.v11i2.18313

Hasanuzzaman, M., Azad, M. A. K., & Hossain, M. M. (2021). Effects of Dufour and thermal diffusion on unsteady MHD free convection and mass transfer flow through an infinite vertical permeable sheet. SN Applied Sciences, 3(12), 882.https://doi.org/10.1007/s42452-021-04842-8

Hossain, M., Nasrin, R., & Hasanuzzaman, M. (2022). Radiative and MHD Effects on Time-Dependent Thermal-Material Transfer by Micropolar Binary Mixture. Advances in Mathematical Physics, 2022. https://doi.org/10.1155/2022/2224435

Kalpana, G., Madhura, K. R., & Kudenatti, R. B. (2019). Impact of temperature-dependant viscosity and thermal conductivity on MHD boundary layer flow of two-phase dusty fluid through permeable medium. Engineering Science and Technology, an International Journal, 22(2), 416-427. https://doi.org/10.1016/j.jestch.2018.10.009

Khan, W., Idress, M., Gul, T., Khan, M. A., & Bonyah, E. (2018). Three non-Newtonian fluids flow considering thin film over an unsteady stretching surface with variable fluid properties. Advances in Mechanical Engineering, 10(10), 1687814018807361, https://doi.org/10.1177/1687814018807361

Machireddy, G. R., & Naramgari, S. (2018). Heat and mass transfer in radiative MHD Carreau fluid with cross diffusion. Ain Shams Engineering Journal, 9(4), 1189-1204. https://doi.org/10.1016/j.asej.2016.06.012

Madhura, K. R., Babitha, & Iyengar, S. S. (2022). Numerical investigation on magnetohydrodynamics boundary layer flow of micropolar Carreau nanofluid with nonlinear thermal radiation. International Journal of Ambient Energy, 43(1), 6224-6232. https://doi.org/10.1080/01430750.2021.2009370

Makinde, O. D. (2011). On MHD mixed convection with Soret and Dufour effects past a vertical plate embedded in a porous medium. Latin American applied research, 41(1), 63-68.

Nasrin, R. (2010): MHD free convection flow along a vertical flat plate with thermal conductivity and viscosity depending on temperature, Journal of Naval Architecture and Marin Engineering, Vol. 6, No. 2. https://doi.org/10.3329/jname.v6i2.4994

Nasrin. R and Alim, M.A. (2010): Combined effects of viscous dissipation and temperature dependent thermal conductivity on MHD free convection flow with conduction and joule heating along a vertical flat plate, Journal of Naval Architecture and Marin Engineering, Vol. 6, No. 1. https://doi.org/10.3329/jname.v6i1.2648

Pramanik, S. (2014). Casson fluid flow and heat transfer past an exponentially porous stretching surface in presence of thermal radiation. Ain shams engineering journal, 5(1), 205-212. https://doi.org/10.1016/j.asej.2013.05.003

Priam, S. S., & Nasrin, R. (2022). Numerical appraisal of time-dependent peristaltic duct flow using Casson fluid. International Journal of Mechanical Sciences, 233, 107676. https://doi.org/10.1016/j.ijmecsci.2022.107676

Raju, C. S. K., & Sandeep, N. (2016). Unsteady three-dimensional flow of Casson-Carreau fluids past a stretching surface, Alexandria Eng. J, 55(2), 1115-1126. https://doi.org/10.1016/j.aej.2016.03.023

Reddy, J. R., Kumar, K. A., Sugunamma, V., & Sandeep, N. (2018). Effect of cross diffusion on MHD non-Newtonian fluids flow past a stretching sheet with non-uniform heat source/sink: A comparative study. Alexandria engineering journal, 57(3), 1829-1838.https://doi.org/10.1016/j.aej.2017.03.008

Seethamahalakshmi, V., Murthy, C. V. R., & Reddy, G. V. R. (2020). Influence of Radiation and chemical reaction on MHD Casson Nanofluid on a stretching sheet. In Diffusion Foundations (Vol. 28, pp. 57-64). Trans Tech Publications Ltd. https://doi.org/10.4028/www.scientific.net/DF.28.57

Shah, R. A., Abbas, T., Idrees, M., & Ullah, M. (2017). MHD Carreau fluid slip flow over a porous stretching sheet with viscous dissipation and variable thermal conductivity. Boundary Value Problems, 2017(1), 94. https://doi.org/10.1186/s13661-017-0827-4

Sharma, B. K., Gupta, S., Krishna, V. V., & Bhargavi, R. J. (2014). Soret and Dufour effects on an unsteady MHD mixed convective flow past an infinite vertical plate with Ohmic dissipation and heat source. Afrika Matematika, 25, 799-821. https://doi.org/10.1007/s13370-013-0154-6

Sharma, R. P., Tinker, S., Gireesha, B. J., & Nagaraja, B. (2020). Effect of convective heat and mass conditions in magnetohydrodynamic boundary layer flow with Joule heating and thermal radiation. International Journal of Applied Mechanics and Engineering, 25(3), 103-116. https://doi.org/10.2478/ijame-2020-0037

Siddabasappa, C. (2020). Unsteady magneto-hydrodynamic flow through saturated porous medium with thermal non-equilibrium and radiation effects. International Journal of Applied and Computational Mathematics, 6, 1-23. https://doi.org/10.1007/s40819-020-00825-2

Siddabasappa, C., Siddheshwar, P. G., & Makinde, O. D. (2021). A study on entropy generation and heat transfer in a magnetohydrodynamic flow of a couple-stress fluid through a thermal nonequilibrium vertical porous channel. Heat Transfer, 50(6), 6377-6400. https://doi.org/10.1002/htj.22176

Uddin, M. J., & Nasrin, R. (2023). A Numerical Assessment of Time-Dependent Magneto-Convective Thermal-Material Transfer over a Vertical Permeable Plate. Journal of Applied Mathematics, 2023. https://doi.org/10.1155/2023/9977857

Waqas, H., Hussain, S., Naseem, R., Mariam, A., & Khalid, S. (2017). Mixed Convection and Radiative Heat Transfer of MHD Casson Fluid Flow by a Permeable Stretching Sheet with Variable Thermal Conductivity and Lying in Porous Medium. British Journal of Mathematics & Computer Science, 22(6), 1-14. https://doi.org/10.9734/BJMCS/2017/33762